RAPID COMMUNICATIONS

PHYSICAL REVIEW B VOLUME 48, NUMBER 14 1 OCTOBER 1993-II

Superlubricity of molybdenum disulphide

J. M. Martin, C. Donnet, and Th. Le Mogne
Département de Technologie des Surfaces, Ecole Centrale de Lyon, Laboratoire de Tribologie et Dynamique des Systèmes, Boîte Postale 163, 69131 Ecully Cedex, France

Th. Epicier
Institut National des Sciences Appliquées de Lyon, Groupe d'Études de Métallurgie Physique et de Physique des Matériaux, 69621 Villeurbanne Cedex, France

(Received 15 July 1993)

We have studied the atomistic origins of the ultralow friction coefficient of a molybdenum disulphide (MoS_2) coating in ultrahigh vacuum conditions. A friction coefficient in the 10^{-3} range is associated with friction-induced orientation of "easy shear" basal planes of the MoS_2 crystal structure parallel to the sliding direction. In addition to this basal plane orientation, an orientation disorder around the c axis is observed, indicating that frictional anisotropy during intercrystallite slip could be at the origin of the vanishing of the friction force. Experimental HRTEM lattice fringe imaging of MoS_2 wear particles clearly show the existence of characteristic Moiré patterns. We have simulated TEM lattice fringe images of a [0001] MoS_2 crystal and produced rotational Moiré patterns by superimposing two such images. A qualitative agreement between experimental and simulated Moiré patterns is demonstrated, which gives credence that ultralow friction of MoS_2 in high vacuum can be attributed to a superlubric situation, by frictional anisotropy of sulphur-rich basal planes during intercrystallite slip.

Superlubricity is the state in which two contacting surfaces exhibit no resistance to sliding. Shinjo and Hirano have shown that superlubricity is related to the atomistic origin of friction and that the phenomenon appears when the sum of the force on each moving atom against the entire system vanishes. A specific case of superlubric situation is frictional anisotropy[2] when incommensurate contacting surfaces are sliding on each other, which can be the case of two contacting crystal lattices at a certain misfit angle. The existence of superlubricity has been recently suggested for an hexagonal symmetry of the crystal: experiments were carried out by measuring friction between two contacting surfaces of cleaved mica, when changing the lattice misfit angle.[3] The friction force can be lowered by one order of magnitude. However, no frictional anisotropy could be seen in ambient atmosphere, showing that the absence of surface contaminants is a determinant factor to reach the superlubric state. However, no direct experimental evidence for this mechanism has been given by the authors.

Molybdenum disulphide (MoS_2) is a well-known lamellar solid lubricant with a hexagonal structure and extensive surveys exist in the literature.[4–7] Ultralow friction of MoS_2 coatings in practical situations has been recognized when running friction tests in the absence of water vapor, either in an inert gas or in high vacuum (Fig. 1). Under such experimental conditions, and depending upon the normal load, friction coefficients between 0.01 and 0.05 have been measured, which already represents uncommon values in solid film lubrication.[5] Recently,[8] using a dedicated ultrahigh vacuum analytical tribotester, it has been found that friction could be lowered by one order of magnitude (10^{-3} range) when testing a sputtered MoS_2 coating exempt of impurities such as carbon, oxygen, and water vapor.

The mechanisms of ultralow friction of MoS_2 have already been studied in the literature[5] and low friction needs the three following conditions to be satisfied:

(1) Built-in of a MoS_2 *transfer film* on the frictional counterface. This transfer film is formed owing to a good adhesion of MoS_2 to the antagonist material. The film does not transfer immediately but very progressively: thin atomic layers originating at the flat are compact, so that the film thickness on the flat itself is hardly affected because of the extensive difference in the kinematic lengths.

(2) *Friction-induced reorientation of the (0001) basal planes* of the MoS_2 grains in the interface occurs parallel to the sliding direction (in the transfer film, the film itself and eventually the third bodies in general). It is anticipated that friction-induced basal orientation occurs very early at the beginning of sliding, by a simultaneous switching of all the individual nanometer-scale MoS_2 grains in the interface.

(3) *Absence of contaminants.* MoS_2 coatings often contain oxygen, either as molybdenum oxide or in substitution of sulphur atoms in the lamellar structure[9] so that the crystal lattice can be modified by the presence of oxygen. Carbon is also a well-known contaminant of MoS_2, coming from the residual gas during the sputtering pro-

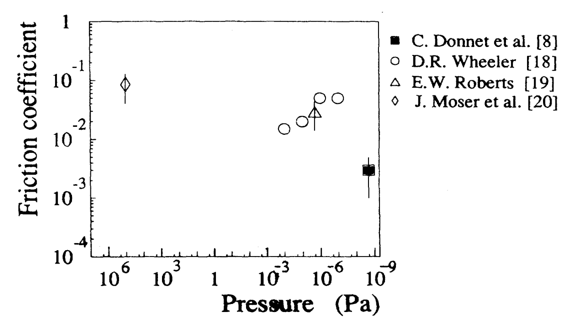

FIG. 1. Friction coefficient of PVD MoS_2 coatings vs environmental pressure, from Refs. 8 and 18–20.

cess. Special attention must be paid to the effect of water vapor coming from the ambient air or from a humid environment during storage, for example. It has been suggested that liquid water could be formed by capillarity condensation in the defects of the MoS_2 crystal structure and that water would then modify the easy shear between basal planes.[10]

Considering the theoretical basis proposed by Hirano, we suspect that pure and stoichiometric MoS_2 should satisfy the condition of superlubricity in the absence of any contamination (in high vacuum or an inert atmosphere), by *frictional anisotropy of the shear-oriented low-energy basal planes.*

An experimental study was carried out by using the ultrahigh vacuum analytical tribometer coupled to a preparation chamber, which has already been described in detail earlier.[11] With this apparatus, a sputter-deposited oxygen-free MoS_2 coating can be obtained on a solid substrate, and transferred to a pin-on-flat friction machine without breaking vacuum. Under these conditions, it has been possible to study the relation between the utlralow friction of MoS_2 and the crystal structure of the transfer film in the sliding interface. The friction-oriented microstructure of the interface material (mainly as wear fragments) was investigated by electron diffraction in the selected area mode (SAED) and by high resolution transmission electron microscopy (HRTEM) using a 400-kV accelerating voltage TEM, in order to examine the structure of the interface material at the atomic scale.

Radio-frequency (rf) magnetron sputtering of MoS_2 was performed on a cleaned bearing steel (AISI 52100) surface at room temperature, using a previously degassed MoS_2 target. A 120-nm-thick film was obtained by sputtering MoS_2 at 7.4 W/cm^2 with a current intensity of 300 mA. An *in situ* analysis of the coating was performed by x-ray photoelectron spectroscopy. The Mo $3d5/2$ and $S2p3/2$ signals were, respectively, centered at 228.8 ± 0.2 eV and 162.0 ± 0.2 eV, in agreement with already published values corresponding to MoS_2.[12] The chemical composition of the film was calculated using the Mo $3d$ and $S2p$ peak intensities and sensitivity factors published by Briggs and Seah.[13] The experimental S:Mo ratio was 2.04, thus suggesting the film to be nearly stoichiometric. Auger Electron Spectroscopy analyses did not show any trace of contamination element such as carbon or oxygen, within the detection limits of the technique.

The friction measurements were carried out using a reciprocating pin-on-flat tribometer. A hemispherical pin fixed on a horizontal arm is connected to the UHV chamber by a double cantilever spring device. When a force is applied, the spring's elastic deformation is measured and converted to a force via a noncontacting transducer (LVDT) after a calibration procedure.

The difficulty in measuring ultralow friction in high vacuum must be emphasized here . The calibration of the tangential force was carried out in vacuum using an electromagnetic device. The analog-digital converter allows a minimal recorded force of 5.10^{-4} N. The noise (electronic plus mechanical) does not exceed a few millinewtons. Consequently, the minimal average friction force which is detectable with the equipment at hand is about 2.10^{-3} N, corresponding to a friction coefficient of 2.10^{-3} for a 1-N normal load.

A stepper motor generates a linear reciprocating motion of the flat in the x-axis direction. The mean value of the friction tangential force over one cycle can be obtained by calculating the average value of the signal between two consecutive passes of the pin on the flat, and dividing by two. The contribution of the signal originating from the extremities of the wear track is neglected. The friction coefficient for each cycle is given by the ratio of the tangential force to the normal load.

The tribological parameters of the reciprocating pin-on-flat machine were the following: using a steel hemispherical pin (4-mm-radius curvature) as a hard material, and several identical MoS_2-on-steel coatings, we performed 50-cycle tests with a normal load of 1.2 N, corresponding to a mean contact pressure of 0.4 GPa, a linear sliding speed of 0.5 mm/s and a 3 mm wear track length. The residual pressure in the test chamber was 50 nPa (5.10^{-10} torr).

Figure 2(a) shows the typical evolution of the average friction coefficient, as a function of the number of cycles during the test. At the beginning, the friction coefficient is 0.01 but it drastically decreases to the 0.001 range a few cycles later. Negative values arise from the calculation indicating that, in this case, the noise can be larger than the signal from the transducer. At this stage, we practically observe a vanishing of the friction force, which has never been observed before. Figure 2(b) shows a detail of the unprocessed friction tangential force recorded over one cycle (two alternate passes of the pin on the flat in cycle number 22), during a very low friction regime in the test. As can be seen, the friction force change in direction can hardly be detected during this cycle; only the unfiltered natural resonance frequency (approximately 16 Hz) from the elastic cantilever is detected. Ten oscillations are observed in Fig. 2(b), thus indicating a complete vanishing of the friction force in the contact. In other cases, the stabilized friction coefficient did not completely vanish, but the values were always below 0.005.[8]

HRTEM experiments have been conducted on MoS_2 wear debris. At the end of the friction test, some wear fragments from the flat were collected on a holey carbon film mounted on a copper grid, and examined in a 4000EX JEOL microscope operating at 400 kV. [0001] multibeam images were recorded with an objective aperture limiting the interferences to the $\{10\bar{1}0\}$ reflections [see Fig. 3 (a)], corresponding to the prismatic planes with an inter-reticular distance $d\{10\bar{1}0\}=0.2737$ nm. Under such imaging conditions, the atomic structure of MoS_2 cannot be fully resolved in the [0001] projection [see Fig. 3(b)]. Indeed, the transfer of the $\{11\bar{2}0\}$ reflections, with $d\{11\bar{2}0\}=0.158$ nm, would be required in order to separate the Mo/S atomic columns [see Figs. 3(c) and 3(d)]; this situation cannot be easily achieved with the 4000EX microscope, which is known to have a point-to-point resolution of 0.17 nm.[17] However, Fig. 3(b) ascertains that the experimental conditions used in

RAPID COMMUNICATIONS

the present study [i.e., such as shown in Fig. 3(a)] are adequate to allow the cell of MoS_2, projected onto the basal plane, to be unambiguously imaged as an hexagonal network of white or black dots, depending upon the actual combination of defocus setting and crystal thickness.

Figure 4(a) is a typical multibeam image obtained from a thin region of a MoS_2 flakelike wear particle, and taken without any specimen tilt in the microscope. Such an image can be commented on as follows.

(i) The numerical diffractogram of Fig. 4(a) (shown as inset) indicates a microcrystalline structure with a very small grain size [i.e., a nanometer size—see (ii)]. Moreover, the (0002) ring is missing, which definitely confirms that the MoS_2 grains have been oriented by friction, with their basal planes parallel to the sliding direction, as already reported in the literature.[7,8] More interesting here is the evidence that those crystallites do not have the same orientation, since a "quasicontinuous" ring is observed.

(ii) Small nanometer-sized domains are clearly observed, which correspond to the hexagonal network depicted in Fig. 3(b) imaged with a "normal" or "reverse"

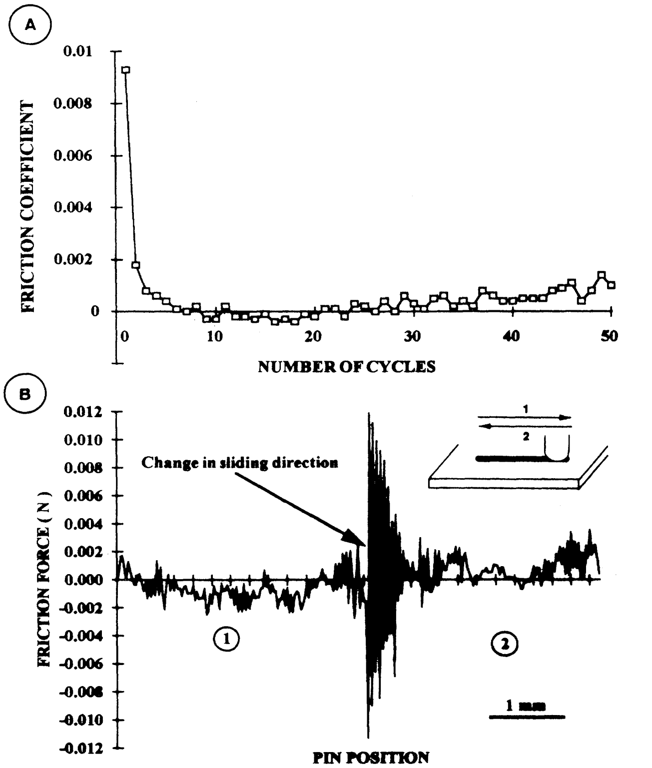

FIG. 2. Superlow friction of MoS_2 in high vacuum. (a) Evolution of the average friction coefficient as a function of the number of cycles. The vanishing of the friction force is observed after 7 cycles. Negative values arise from the fact that the noise can be larger than the signal. (b) Detail of the friction force recorded during the cycle number 22. The noise represents a few millinewtons but the change in the sliding direction cannot be detected. The average friction force is calculated by averaging the signal on the two consecutive passes 1 and 2, and dividing by two. The friction coefficient over 1 cycle is obtained by making the ratio between the friction force and the normal load (1.2 N).

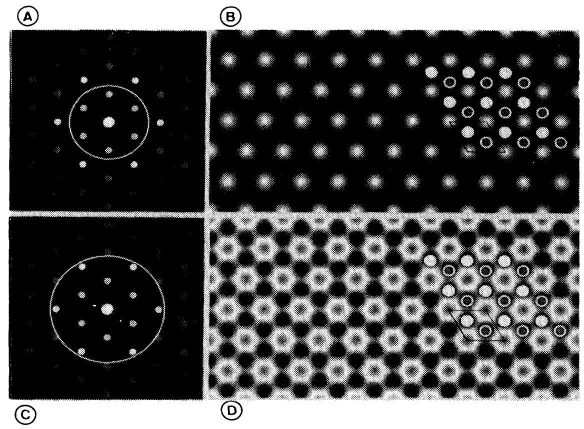

FIG. 3. TEM simulated images of a [0001] MoS_2 crystal [simulations have been run with SIMPLY (Ref. 14), a PC software including the SHRLI programs (Ref. 15)]. (a) Calculated diffraction pattern of a one-cell thick crystal of MoS_2 [hexagonal structure $P6_3/mmc$, with $a=0.3164$ and $c=1.2295$ nm (Ref. 16)]. The circle represents the position of the objective aperture used in the present HRTEM study. (b) "Weak-phase-object" image corresponding to (a). The atomic projection of MoS_2 is superimposed on the simulated image (white and grey circlers correspond to Mo and S atoms, respectively; all atomic columns consist in a succession of both kinds of atoms). (c) and (d) Simulations corresponding to (a) and (b), respectively, for a larger objective aperture (see text).

contrast. The orientation of those hexagonal networks varies from place to place, which indicates that the domains exhibit a rotational disorder around their common c axis. Between the domains, the dot contrast frequently vanishes, which is due to the production of Moiré patterns, as clearly illustrated in Figs. 4(b) and 4(c): these enlargements show two details from a thin region of the flat MoS_2 wear fragment with $\{10\bar{1}0\}$ lattice fringes ([0001] common axis). Moiré patterns, underlined by the coincidence lattice domains, are observed very clearly. Using an image analyzer and a fast Fourier transform (EFT) algorithm, numerical diffractograms of these two regions have been obtained [shown as inset in Figs. 4(b) and 4(c), respectively]. It is seen that both regions do contain two main distinct [0001] orientations, and the misfit angle can be measured in each case. Figures 4(d) and 4(e) are Moiré patterns reconstructed numerically, by adding two HRTEM simulated images, such as Fig. 3(b), with misfit angles corresponding to those measured from the diffractograms in Figs. 4(b) and 4(c). A qualitative agreement between the experimental [Figs. 4(b) and 4(c)] images and the calculated ones [Figs. 4(d) and 4(e)] is obtained (differences arise from the local distortions and noise signal present in the experimental images). In our opinion, this agreement gives a strong evidence for superlubricity of MoS_2 by frictional anisotropy. A more systematical and statistical study of angular misfits between nanometer-sized MoS_2 crystallites in the wear interface layer is in progress.

We have studied the *in vacuo* tribological properties of rf-magnetron sputtered MoS_2 coatings deposited on cleaned bearing steel surfaces, using a UHV AES/XPS tribometer previously developed. The films were *in-situ* prepared and transferred to the test chamber without breaking vacuum. Using the reciprocating pin-on-flat analytical tribometer, great care was taken to measure very low friction coefficients accurately, by optimizing the data processing and the calibration procedure of the friction force.

The friction coefficient exhibited by the MoS_2 coating *in vacuo* was extraordinary low. The calculated average value on each cycle was below 0.002 and in some cases the tangential force was hardly detected as if the friction force completely vanished.

Friction-induced orientation of the MoS_2 grains in the contact interface was clearly demonstrated by electron diffraction and high resolution TEM studies, carried out on selected wear debris collected at the end of the friction test. It is interesting to note that the orientation does not affect the other crystallographic directions which remained unchanged.

High resolution TEM images performed on wear fragments clearly demonstrate the existence of Moiré patterns corresponding to the presence of superimposed MoS_2 crystals with a rotation angle between them. This is confirmed by computer-simulated Moiré patterns obtained from two superimposed basal planes of the hexagonal lattice. The local misfit angle can be easily measured by FFT carried out directly on the images.

Considering the recent theoretical basis proposed by Hirano, the vanishing of the friction force in high vacuum is attributed to a superlubric state, by frictional anisotropy of friction-oriented sulphur basal planes of MoS_2 grains during intercrystallite slip.

Future works will involve the study of the conservation of superlubricity of MoS_2 in a nitrogen atmosphere, and the effects of partial pressures of oxygen and water vapor, in order to stimulate the space environment with regard to practical applications.

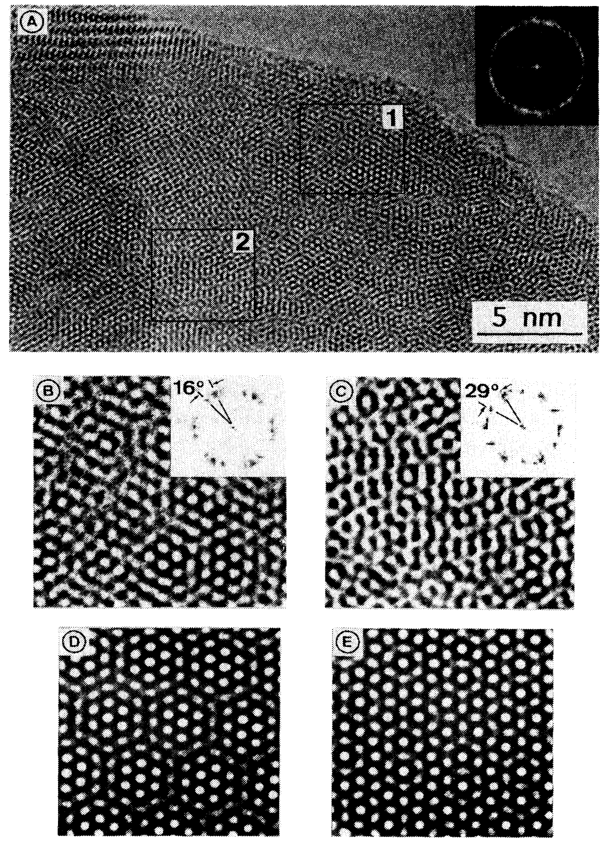

FIG. 4. Imaging of MoS_2 wear particles. (a) general view; the inset diffractogram, obtained from the central area, shows a quasicontinuous $\{10\bar{1}0\}$ ring. (b) and (c) Enlarged frames labeled 1 and 2 in (a). Inset diffractograms are displayed in reverse contrast for a better visibility (see text for comments). (d) and (e) Numerical Moiré patterns corresponding to the angular misfits measured for experimental images (b) and (c), respectively.

The authors would like to thank A. Tonck for his help on the friction force device and M. N. Gardos and P. Fleischauer for helpful comments and discussions. The HRTEM experiments were performed on the 400 kV microscope at the CENG (Centre d'Etudes Nucléaires de Grenoble, France), which is here acknowledged. Laboratoire de Tribologie et Dynamique des Systèmes is Unité Associée No. 855 of CNRS and Groupe d'Etudes de Métallurgie Physique et de Physique des Matériaux is Unité Associée No. 341.

[1]K. Shinjo and M. Hirano, Surf. Sci. **283**, 473 (1993).
[2]J. B. Sokoloff, Phys. Rev. B **42**, 760 (1990).
[3]M. Hirano, K. Shinjo, R. Kaneko, and Y. Murato, Phys. Rev. Lett. **67**, 2642 (1991).
[4]T. Spalvins, J. Vac. Sci. Tech. A **5**, 212 (1987).
[5]E. W. Roberts, Tribol. Int. **23**, 95 (1990).
[6]I. L. Singer, *Fundamental in Friction: Macroscopic and Microscopic Processes,* edited by I. L. Singer and H. M. Pollock (Kluwer, Academic, Dordrecht, Netherlands, 1992), p. 237.
[7]P. D. Fleischauer and R. Bauer, Tribol. Trans. **31**, 239 (1988).
[8]C. Donnet, T. Le Mogne, and J. M. Martin, *International Conference on the Metallurgical Coatings and Thin Films,* San Diego, 1993 [Surf. Coat. Tech. (to be published)].
[9]J. R. Lince, M. R. Hilton, and A. S. Bommannavar, Surf. Coat. Tech. **43/44**, 640 (1990).
[10]M. Uemura, K. Saito, and K. Nakao, Tribol. Trans. **33**, 551 (1990).
[11]J. M. Martin and T. Le Mogne, Surf. Coat. Tech. **49**, 427 (1991).
[12]T. B. Steward and P. D. Fleischauer, Inorg. Chem. **21**, 2426 (1982).
[13]D. Briggs and M. P. Seah, *Practical Surface Analysis by Auger and X-Ray Electron Spectroscopies* (Wiley Science, New-York, 1985).
[14]T. Epicier and M. A. O'Keefe (unpublished).
[15]M. A. O'Keefe, P. R. Buseck, and S. Iijima, Nature **274**, 322 (1978).
[16]A. A. Balchin, in *Crystallography and Crystal Chemistry of Materials with Layered Structures,* edited by F. Levy (Reidel, Dordrecht, 1976), p. 1-50.
[17]A. Bourret and J. M. Penisson, JEOL News **25E**, 2 (1987).
[18]D. R. Wheeler, Thin Sol. Films **223**, 78 (1993).
[19]E. W. Roberts, Tribol. Int. **23**, 95 (1990).
[20]J. Moser and F. Levy, J. Mater. Res. **8** 206 (1993).

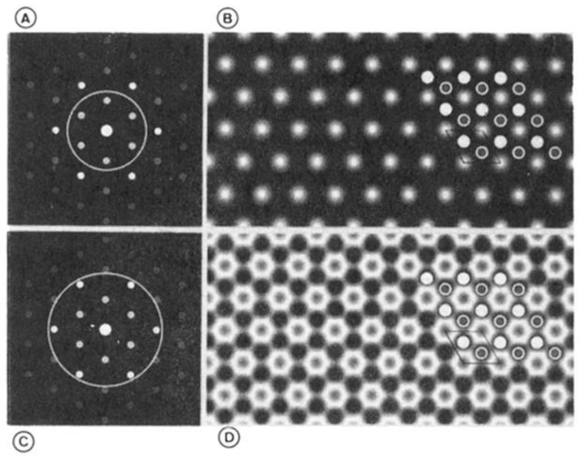

FIG. 3. TEM simulated images of a [0001] MoS_2 crystal [simulations have been run with SIMPLY (Ref. 14), a PC software including the SHRLI programs (Ref. 15)]. (a) Calculated diffraction pattern of a one-cell thick crystal of MoS_2 [hexagonal structure $P6_3/mmc$, with $a = 0.3164$ and $c = 1.2295$ nm (Ref. 16)]. The circle represents the position of the objective aperture used in the present HRTEM study. (b) "Weak-phase-object" image corresponding to (a). The atomic projection of MoS_2 is superimposed on the simulated image (white and grey circlers correspond to Mo and S atoms, respectively; all atomic columns consist in a succession of both kinds of atoms). (c) and (d) Simulations corresponding to (a) and (b), respectively, for a larger objective aperture (see text).

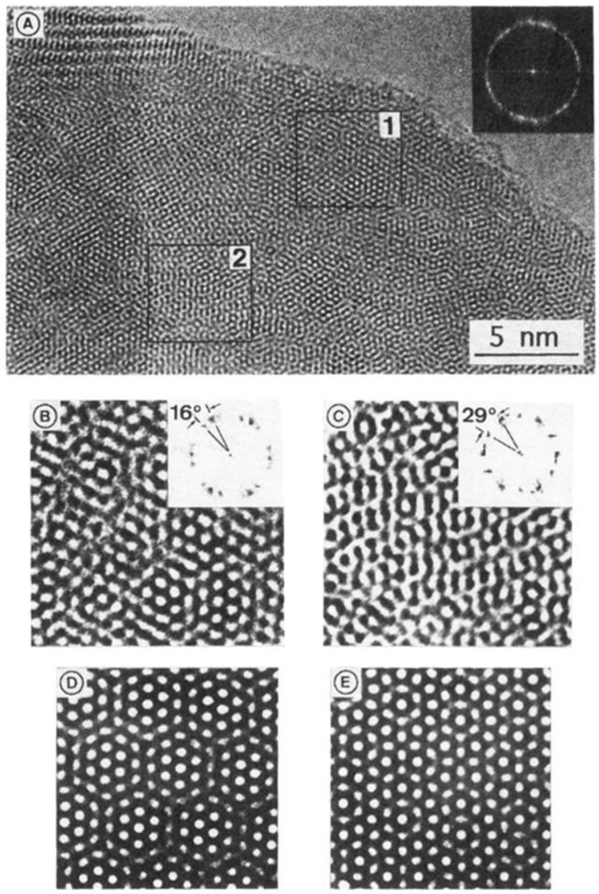

FIG. 4. Imaging of MoS_2 wear particles. (a) general view; the inset diffractogram, obtained from the central area, shows a quasicontinuous {1010} ring. (b) and (c) Enlarged frames labeled 1 and 2 in (a). Inset diffractograms are displayed in reverse contrast for a better visibility (see text for comments). (d) and (e) Numerical Moiré patterns corresponding to the angular misfits measured for experimental images (b) and (c), respectively.